Davies, J. M., 2023: Supercell Tornado Lead Time and Low-level Lapse Rates. *Electronic J. Severe Storms Meteor.*, _ (_), _–_.

Electronic Journal of
SEVERE STORMS METEOROLOGY

Supercell Tornado Lead Time and Low-level Lapse Rates

JONATHAN M. DAVIES
Kansas City, MO

(Submitted 21 January 2023)

ABSTRACT

On some days when well-anticipated tornado outbreaks occur in environments supporting tornadic supercells, there is a delay of several hours before development of tornadoes with the initial storms. To explore the slow beginning of some tornado events and outbreaks, this empirical study looks at low-level lapse rates (specifically, *0–3-km lapse rates*, a potential contributor to low-level stretching in storm updrafts) as a possible significant factor relating to *tornado lead time* in tornadic supercells (defined as the time from the first 40 dBZ core on radar to the first tornado). Using radar data in 103 tornadic supercell cases from late 2021 through late 2022, Storm Prediction Center mesoscale analysis products were examined comparing 0–3-km lapse rates to tornado lead time. Because steeper low-level lapse rates tend to be associated with heating over elevated terrain, geographical location from east to west across the U.S. was also considered. Results show that tornadic supercells in the eastern U.S. tend to take longer to produce tornadoes. Faster tornado development tends to occur with supercells in steeper lapse rate environments, particularly in the High Plains and at times the central Plains of the U.S. Because public perception of urgency on dangerous tornado days can be adversely affected by early false alarm warnings (the 10 December 2021 Mayfield, KY case is reviewed as an example), information from this study has application to warning decision making, especially in the early stages of tornado episodes and outbreaks.

1. Introduction

In some tornado outbreaks, several hours may pass before initial supercell storms that form go on to produce tornadoes. A recent example was the 29–30 November 2022 tornado outbreak in the southern U.S. where, *before* any tornadoes were confirmed, 18 tornado warnings based on radar-indicated rotation were issued on 29 November 2022 between 1742 UTC and 2204 UTC. These were for several separate supercell storms from eastern Texas to Louisiana and Mississippi, a period of more than *four hours*.

Figure 1 at early afternoon on 29 November 2022 shows the effective-layer significant tornado parameter (STP, Thompson et al. 2004) from the Storm Prediction Center (SPC) mesoscale analysis (Bothwell et al. 2002; Storm Prediction Center 2014).

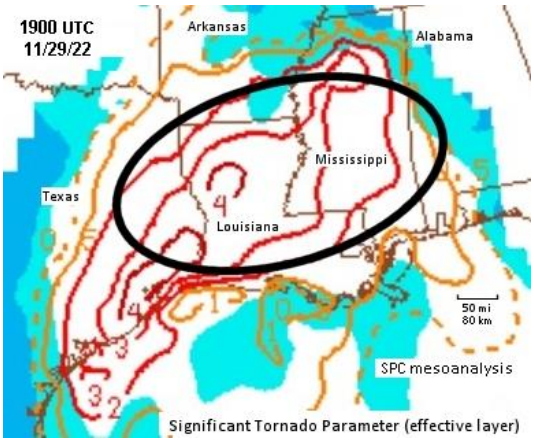

Figure 1: STP (effective layer, no dimensions, red contours) from SPC mesoanalysis at 1900 UTC on 29 November 2022, mixed-layer convective inhibition in blue shading (light > 25 J kg^{-1}; dark > 100 J kg^{-1}). Ellipse is area where 18 tornado warnings were issued before any verification between 1742 UTC and 2204 UTC.

Corresponding author address: Jon Davies, Kansas City, MO, E-mail: davieswx@gmail.com

From this graphic, the background environment appeared quite supportive of tornadoes over several southern U.S. states. But within the area in Fig. 1 indicated by the black ellipse, many unverified tornado warnings were issued prior to 2200 UTC, well before the first confirmed tornadoes.

Why this delay in tornado production for storms within a favorable environment for supercell tornadoes? Events like this are a motivation for this study, and are not a trivial issue. For example, an early false alarm tornado warning in Kentucky at Mayfield, before the start of the deadly 10 December 2021 tornado outbreak and four hours before a large tornado struck the town (Fig. 2) may have contributed to lives lost (El-Bawab 2021; Hampton 2021; Smith 2021), and will be discussed later in this paper.

Figure 2. Search and rescue efforts at Mayfield Consumer Products candle factory after EF4 tornado struck Mayfield, KY late evening on 10 December 2021 (video image courtesy of Brett Adair/Live Storms Media). Nine people died at the factory. Inset is video image by Eddie Knight showing the tornado later along its path.

In recent years while monitoring tornado events in both real time and post-event study, the author has noted subjectively that, when some storms evolve and go on to produce tornadoes as supercells, temperature lapse rates in the low-levels seem to play a role in how quickly a storm becomes tornadic within a setting favorable for supercell tornadoes. Steeper low-level lapse rates imply potential for stronger near-ground stretching below and within the lower portion of storm updrafts that form in such an environment (Davies 2006a), which can impact tornado development. Hampshire et al. (2017) also found that many higher-rated tornadoes tend to be associated with settings having steeper 0–3-km lapse rates.

This paper will examine radar evolution of over 100 tornadic supercell storms during late 2021 through most of 2022, noting the 0–3-km lapse rate environment from archived SPC graphics (0–3-km lapse rate is a standard product on the SPC mesoanalysis), and also the amount of time from the first notable/established radar core of the storm to the first tornado (the tornado lead time). Geographic differences will also be considered using several areas of the U.S. roughly based on elevation, which has a broad relationship to near-ground lapse rates.

The following section will detail the methodology for this study. Section 3 will present and discuss results. Those results will be applied to several tornado cases in section 4, including the aforementioned 10 December 2021 Mayfield, KY setting that involved an early false alarm tornado warning. The final section is a concluding discussion touching on relevance to short-term forecasting and warning issues.

2. Methodology

More than 100 supercell storms that produced tornadoes ranging from EF0 to EF4 in intensity during the one-year period December 2021 through November 2022 were examined using archived composite radar reflectivity images and loops. The tornadic storms were traced backward in the loops at 30 minute intervals to a point where a 40 dBZ composite reflectivity return was first visible (showing up as yellow coloration on most commercial radar displays). The time between this initial radar cell of note and the first tornado produced by the cell, rounded to nearest half hour, was defined as a storm's "*tornado lead time*."

The first 40 dBZ return was chosen as the beginning for approximating tornado lead time because this is halfway between what is considered "light rain" (20 dBZ) and potentially "severe" (60 dBZ) in basic radar meteorology (e.g., National Weather Service 2023). This provided a simple and reasonably consistent starting point early in a storm's life cycle without requiring expert radar interpretation skill. It also would suggest a point at which a storm was becoming established before beginning its evolution into a rotating storm (supercell).

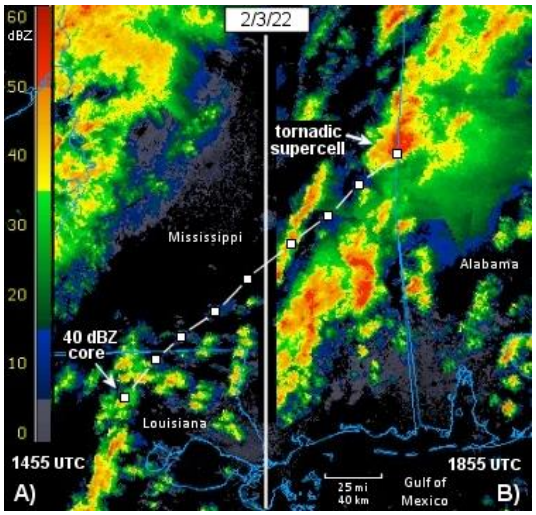

Figure 3. Mosaic of composite radar base reflectivity over southeast Louisiana into southern Mississippi and west-central Alabama on 3 February 2022 at a) 1455 UTC, and b) 1855 UTC. White squares connected by thin white lines show evolution and track of storm that became a tornadic supercell from the approximate time of the first 40 dBZ core in a) to the first tornado in b), at 30 minute intervals.

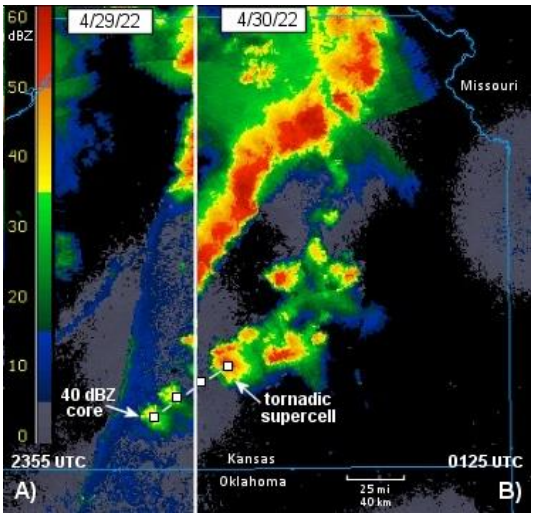

Figure 4. As in Fig. 3, except over central and eastern Kansas at a) 2355 UTC on 29 April 2022, and b) 0125 UTC on 30 April 2022. An EF3 tornado from the tornadic supercell indicated in b) struck Andover, KS after 0110 UTC.

Figures 3 and 4 show examples of this methodology. In Fig. 3, looping backward from a tornadic supercell on 3 February 2022 near the Mississippi/Alabama border that produced an EF2 tornado shortly before 1855 UTC (Fig. 3b), the first 40 dBZ core was found to have originated over southeast Louisiana roughly four hours earlier (Fig. 3a). Figure 4 shows a more discrete supercell in south-central Kansas on 30 April 2022 that spawned an EF3 tornado, striking the town of Andover after 0110 UTC, a few minutes before Fig. 4b. In contrast to the supercell in Fig. 3, this storm took only around 1-1/2 hours after the initial 40 dBZ core (Fig. 4a) to produce a tornado.

Originally, 124 tornadic storms during December 2021 through November 2022 were selected for this study, but 21 cases were discarded because of difficulty in tracking cells on radar due to their origination within squall lines or quasi-linear convective system (QLCS) structures. Eliminating those cases resulted in a total of 103 supercell tornado cases for the database in this study.

Next, archived SPC mesoanalysis graphics were used to estimate 0–3-km lapse rate values near the time and location of the first 40 dBZ core, and also near the time and location of the first tornado produced by the supercell. These values were then averaged to estimate a mean low-level lapse rate over the area traversed by the storm/supercell during its pre-tornadic phase, rather than using a single "snapshot" value near the first tornado.

Figures 5 and 6 (next page) show 0–3-km lapse rate values from the SPC mesoanalysis corresponding to Figs. 3 and 4. The lapse rate near the location of the initial 40 dBZ radar core in southeast Louisiana on 3 February 2022 was approximately 5.2° C km^{-1} (Fig. 5a), and near 5.5° C km^{-1} for the same storm while producing a tornado four hours later (Fig. 5b); the mean 0–3-km lapse rate here was 5.35° C km^{-1} (rounded to 5.4). Similarly, mean low-level lapse rates for the 30 April 2022 Andover, KS supercell during its pre-tornadic phase (Figs. 6a and 6b) were found to be around 7.5° C km^{-1}, much steeper than the environment of the 3 February supercell in Fig. 5 in Mississippi and Alabama.

As mentioned earlier, geographic location was also considered in this study about low-level lapse rates and supercell tornadoes because near-ground lapse rates tend to be steeper in higher terrain during surface heating due to elevation (Davies 2006a) and proximity to

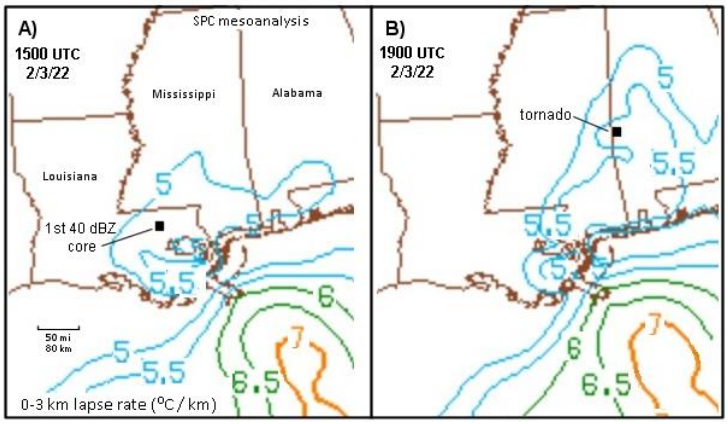

Figure 5. 0–3-km lapse rate (^{o} C km^{-1}) from SPC mesoanalysis on 3 February 2022 at a) 1500 UTC, and b) 1900 UTC, corresponding approximately to radar image times shown in Fig. 3a and 3b. Black squares show locations of first 40 dBZ core, and first tornado, corresponding to Fig. 3a and 3b. Blue contours are lapse rates 5.0 and 5.5, green contours 6.0 and 6.5, and orange contour 7.0.

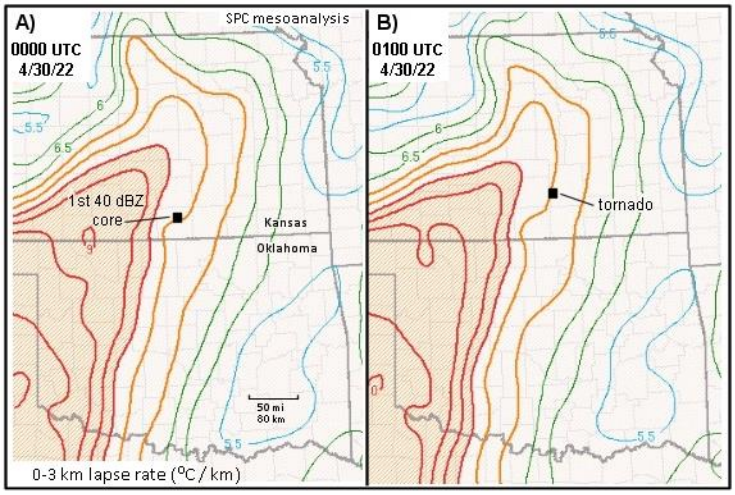

Figure 6. As in Fig 5, except on 30 April 2022 at a) 0000 UTC, and b) 0100 UTC, corresponding approximately to Fig. 4a and 4b. Orange contours are lapse rates 7.0 and 7.5, and red contours and red shading are lapse rates 8.0 and greater.

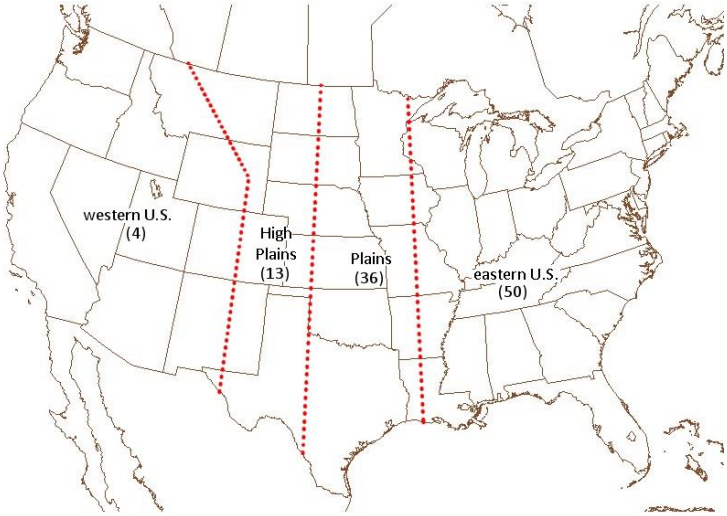

Figure 7. Four U.S. geographic areas used to categorize cases in this study, roughly corresponding to increasing surface elevation from east to west across the U.S. The number of cases in each area is shown in parentheses.

warmer and drier boundary-layer air from the desert southwestern U.S. This was investigated by dividing the U.S. into four areas that in very broad terms correspond to increasing elevation from east to west across the country. Figure 7 (prior page) shows these divisions with lowest elevations in the eastern U.S. (apart from the Appalachian Mountains), increasing elevations in the Plains, higher elevations still in the High Plains just east of the Rocky Mountains, and then the western U.S. with largely mountainous or elevated terrain.

With steeper low-level lapse rates tending to be associated with higher ground-levels above sea level, it might be expected that supercell tornadoes in the Plains, and particularly the High Plains, would tend to develop more quickly with supercells in these areas compared to locations farther east. To see if there is any truth to this idea, Fig. 7 was used to consider supercell tornado cases accordingly by their geographic location. The number of cases located in each area is also shown in Fig. 7.

3. Results

A graphic of averages of the mean 0–3-km lapse rates for supercell tornado cases categorized by tornado lead time at 30 minute intervals (as described in the previous section) is shown using a bar graph in Fig. 8. On the left side of Fig. 8, a strong signal is evident suggesting that supercells established in steeper low-level lapse rate settings (roughly in the 6.5 to 8.5° C km^{-1} range) that then go on to produce tornadoes tend to do so more quickly when compared to lesser low-level lapse rate environments. Longer tornado lead times tend to be associated with 0–3-km lapse rate settings with values around and less than 6.0° C km^{-1}.

Also seen in Fig. 8 when looking at the number of cases associated with each of the tornado lead time half-hour categories, tornado lead times of around two hours and longer were most common (the median lead time for the full database was 2.5 hours, not shown). In fact, when mean 0–3-km lapse rates were less than around 6.0° C km^{-1}, tornado lead times varied considerably, from around two hours to as much as eight hours (not shown explicitly in Fig. 8). On the other hand, of the 21 cases with tornado lead times less than two hours, all but three cases had mean 0–3-km lapse rates greater than 7.0° C km^{-1}.

Not shown in Fig. 8, the smallest 0–3-km lapse rate associated with a supercell tornado in this study was 4.9° C km^{-1} in one case, an EF1 tornado. This suggests that supercell tornadoes may not occur with low-level lapse rates much less than around 5.0° C km^{-1}.

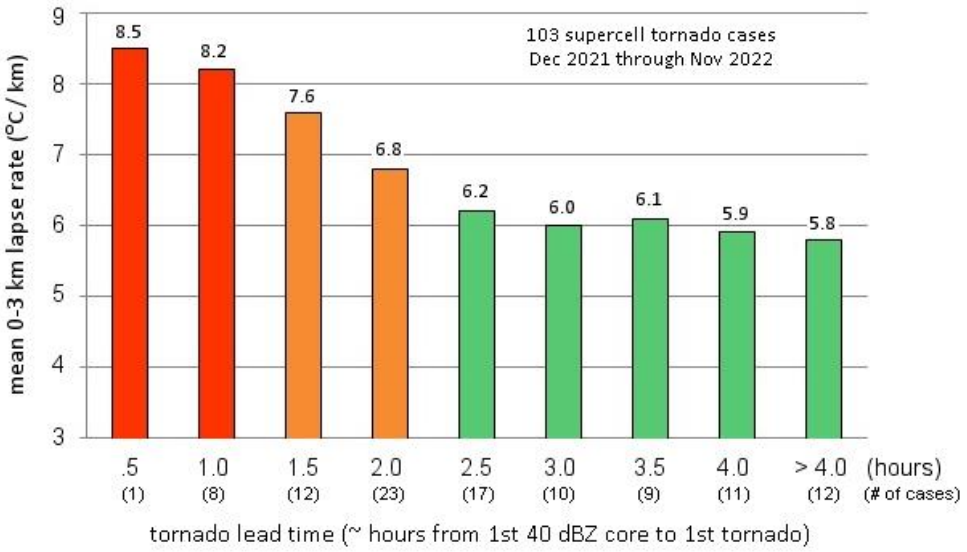

Figure 8. Vertical bar graph showing average 0–3-km mean lapse rate (described in section 2) categorized by tornado lead time (first 40 dBZ radar core to first tornado, rounded to 30 minute intervals) for 103 tornadic supercells examined in this study during December 2021 through November 2022. Red denotes lapse rates > 8.0° C km^{-1}, orange is lapse rates between 6.5 and 8.0, and green is lapse rates < 6.5. Number of cases within each lead time category is shown in parentheses below each bar.

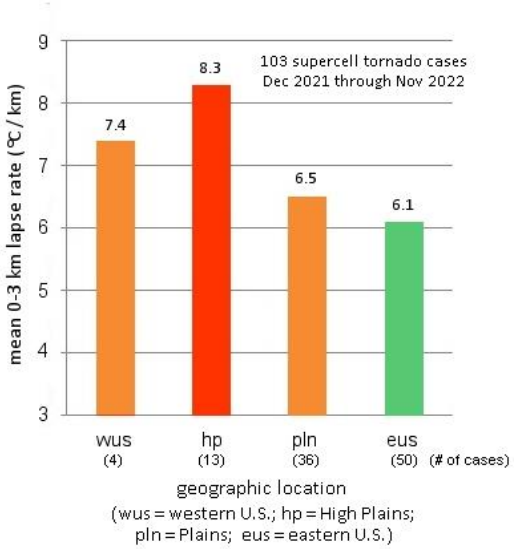

Figure 9. Vertical bar graph showing averages of 0–3-km mean lapse rates associated with the 103 tornadic supercells in Fig. 8 by geographical area in Fig. 7 from section 2.

When examined geographically in Fig. 9, results show that low-level lapse rates in tornadic supercell cases associated with the higher elevations of the western U.S. and, in particular, the High Plains are indeed steeper than in areas farther east. This is as might be expected from discussion in the prior section.

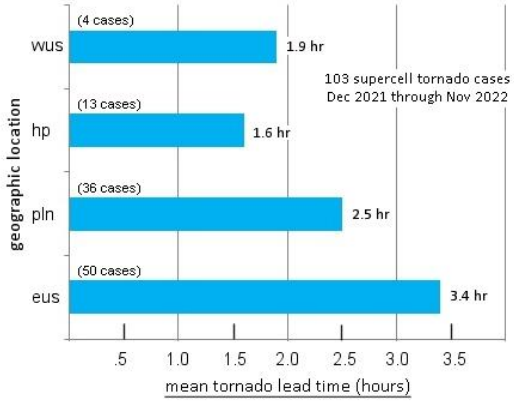

Figure 10. Horizontal bar graph showing mean tornado lead time (time from first 40 dBZ core to first tornado) for the 103 tornadic supercells in Fig. 8 by geographical area in Fig. 7.

From tornado lead time by geographical location in Fig. 10, tornadic supercells in roughly the eastern third of the U.S. (refer back to Fig. 7 in section 2) tend to take the longest time to produce tornadoes, averaging more than 3 hours lead time (the median value was 3.2, not shown). In contrast, tornado lead times in the High Plains and western U.S. tend to be the shortest, likely due in part to the steeper low-level lapse rates associated with higher elevations as seen geographically in Fig. 9.

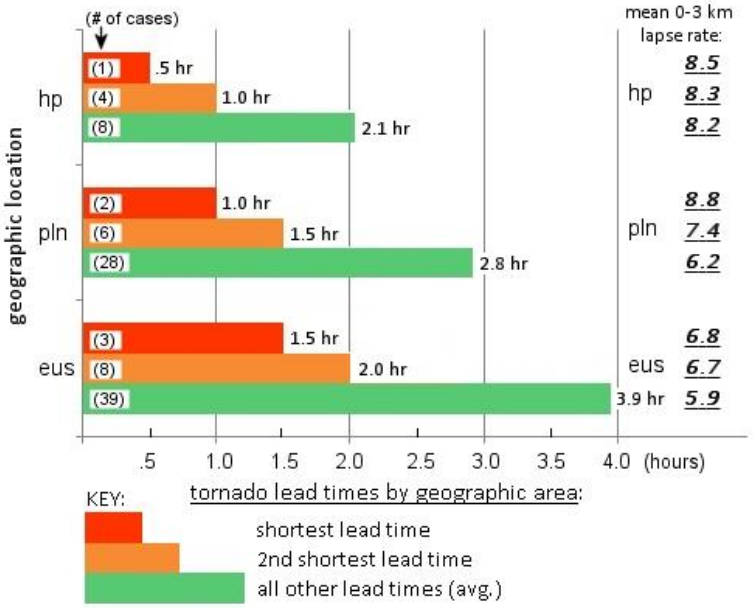

Figure 11. Horizontal bar graph showing tornado lead time similar to Fig. 10, but for the three areas and 99 cases in Fig. 7 east of the Rocky Mountains, broken down into *shortest* lead time (red bars), *second shortest* lead time (orange bars), and the average of all other lead times for that area (green bars). The average of mean 0–3-km lapse rates (^{o}C km^{-1}) associated with each of the categories is shown at right.

Tornado lead times in the Plains east of the High Plains in Fig. 10 tend to fall between those in the eastern U.S. and the High Plains.

With practical and operational application of these results in mind, Fig. 11 (previous page) presents tornado lead times for the three geographical areas east of the Rocky Mountains in Fig. 7 from the prior section (99 cases; four western U.S. cases are removed). Figure 11 is broken down into the first and second *shortest* lead times for each of the three geographical areas compared to an average of all other lead times for that area. This was done to consider the *minimum* lead time from the first notable radar core to the first tornado for supercells within favorable tornado environments in each geographical area, which in turn can impact operational warning issues near the beginning of tornado episodes or outbreaks. Averages of the mean 0–3-km lapse rates associated with each geographical tornado lead time category are also shown on the right side of Fig. 11.

From Fig. 11, the shortest *minimum* tornado lead times with tornadic supercells encountered in this study are in the High Plains at around an hour or less where low-level lapse rates tend to be steepest (8.0^{o} C km^{-1} and higher). In the Plains east of the High Plains, *minimum* lead times tend to be somewhat longer, around 1 to 1.5 hours after the first notable radar core within settings with low-level lapse rates > 6.5^{o} C km^{-1}. Significantly, in the eastern U.S. from the Mississippi River Valley eastward where 0–3-km lapse rates tend to be lower, *minimum* supercell tornado lead times tend to be longer still at around 1.5 to 2 hours, and are often longer.

This has important implications for tornado warning operations. As discussed in the introduction to this paper, the early stages of tornado outbreaks can in some cases involve many rotating storms and tornado warnings *before* tornadoes are reported and verified. False alarm warnings early on during a tornado outbreak day can negatively impact public perception of urgency and awareness as a tornado outbreak progresses. Yet in other situations (e.g., Fig. 4 from section 2), tornadoes may develop relatively quickly from rotating storms, and warning forecasters must be primed to issue effective warnings promptly. The geographical low-level lapse rate results in this study suggest one way to differentiate between some of these contrasting situations when studying the information in Fig. 11.

From the data shown in Fig. 11, Table 1 is a suggested rough reference guideline for *minimum* tornado lead times by geographical area and 0–3-km lapse rate that may be useful when issuing tornado warnings on newly-formed storms that evolve into supercells within an environment forecast to support tornadoes. This general guidance information will be applied to several recent tornado events in the next section.

Table 1.	0-3-km lapse rate ^{o}C km^{-1}	~ ***minimum*** time (hr) from 1st 40 dBZ core to 1st tornado
High Plains (roughly east of Rocky Mountains & west of 100^{o}W longitude)	**≥ 8.0**	**.5 to 1 hr**
	< 8.0	**≥ 1 hr ?**
Plains (roughly east of 100^{o}W longitude & west of Mississippi River Valley)	**≥ 8.0**	**1 to 1.5 hr**
	6.5 - 8.0	**1.5 to 2 hr**
	< 6.5	**≥ 2 hr**
eastern U.S. (roughly Mississippi River Valley & eastward)	**≥ 6.5**	**1.5 to 2 hr**
	< 6.5	**≥ 2 hr**

Table 1. Rough guideline reference table regarding ***minimum*** supercell tornado lead times by U.S. geographic area east of Rocky Mountains (refer to Fig. 7) and 0–3-km lapse rate, derived from Fig. 11 and data in this study.

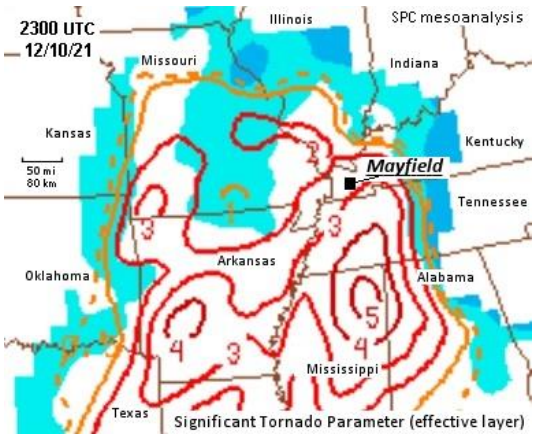

Figure 12. Significant tornado parameter (similar to Fig. 1 in section 1) at 2300 UTC on 10 December 2021, corresponding roughly to radar time in Fig. 13b.

4. Operational application examples

This section will look at how the results from this study might be incorporated into operational use regarding timing of tornado warnings. The first case examined is the Mayfield, KY tornado from the historic 10 December 2021 outbreak mentioned in section 1 that involved an early false alarm tornado warning hours prior to the deadly tornado that struck the town that evening.

a. 10 December 2021 Mayfield, KY tornado

Significant tornadoes were expected over the middle Mississippi River Valley on the evening of 10 December 2021 based on numerous favorable parameters, including the significant tornado parameter from the SPC mesoanalysis (Fig. 12). Before the beginning of the outbreak at 2328 UTC (late afternoon), a radar-based tornado warning was issued for Graves County in western Kentucky, including Mayfield, only about 45 minutes into an early storm's evolution from a 40 dBZ core to a rotating supercell (Fig. 13a and 13b). No tornado occurred with this supercell as it moved south of Mayfield. However, four hours later a large and violent tornado plowed into Mayfield from a supercell that originated during the afternoon over Arkansas, killing and injuring many people.

As suggested in Smith (2021), this early false alarm warning hours well before the EF4 killer tornado may have played a negative role perception-wise regarding safety urgency for some residents of Mayfield, especially those at

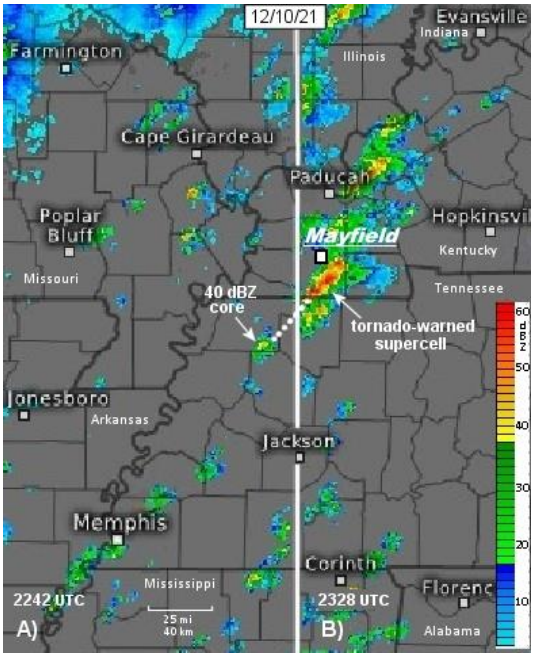

Figure 13. Mosaic of composite radar reflectivity (similar to Figs. 3 and 4) over western Kentucky and Tennessee on 10 December 2021 at a) 2242 UTC, and b) 2328 UTC. Dotted white line shows track of storm discussed in text from first 40 dBZ core in a) to time of false alarm tornado warning in b).

the local candle factory. Employees were allegedly not allowed to take the most effective shelter precautions (e.g., El-Bawab 2021; Hampton 2021) when the deadly tornado approached that evening and a "particularly dangerous situation" tornado warning was issued at 0302 UTC (11 December 2021). Nine people were killed at the factory (see Fig. 2 in section 1), and 15 others died in Mayfield.

Figure 14 (next page) is the 0–3-km lapse rate field from the SPC mesoanalysis at the time of the early false alarm warning, showing low-level lapse rates only in the 5.0 to 5.5^{o} C km^{-1} range over western Kentucky near Mayfield (black square in Fig. 14). Using Fig. 14 and the warning location (eastern U.S.), Table 1 suggests that the *earliest* a tornado might develop from a supercell in this environment would be approximately two hours into its life cycle from an initial 40 dBZ core on radar, rather than 45 minutes to one hour. From the data in this study, the tornado warning issued at 2328 UTC was perhaps too early in the storm's lifetime to reasonably expect a tornado, even though the storm was showing some rotation on radar.

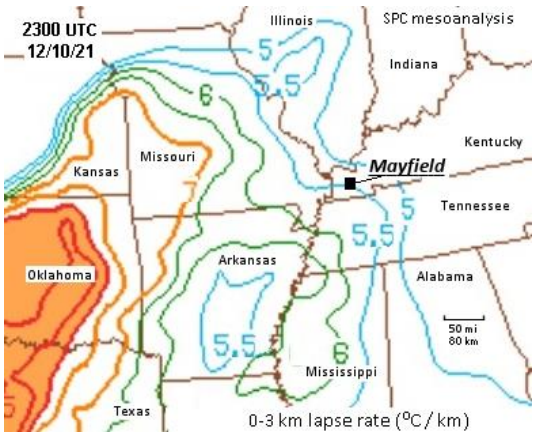

Figure 14. 0–3-km lapse rate as in Fig. 5 from section 2, but at 2300 UTC on 10 December 2021, corresponding to radar time in Fig. 13b.

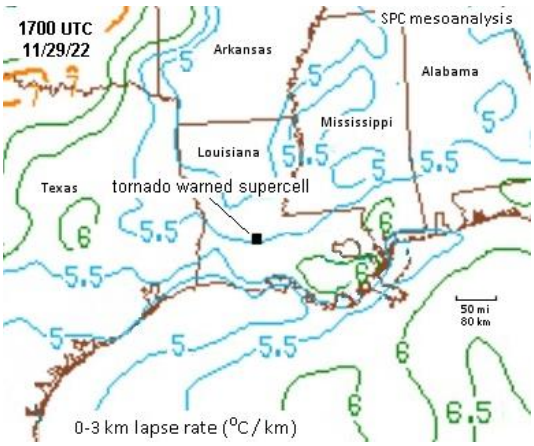

Figure 15. As in Fig. 14, except at 1700 UTC on 29 November 2022, a couple hours before Fig. 1 from section 1. Black square shows location of first tornado-warned supercell.

b. 29 November 2022 southern U.S. tornado outbreak

This case was also mentioned in section 1 (see Fig. 1). The first tornado warning was issued at 1742 UTC in south-central Louisiana (see location of black square in Fig. 15) on this "moderate risk" severe weather day as outlooked by SPC with tornado potential centered on portions of Louisiana and Mississippi.

Figure 15 also shows 0–3-km lapse rates from the SPC mesoanalysis around the time this first tornado warning was issued. Notice that low-level lapse rates across most of Louisiana and Mississippi were less than 6.0^{o} C km^{-1}. Using the eastern U.S. section of Table 1, this suggests that, as with the prior case above, the *earliest* a tornado might develop from a supercell in this environment would be around two hours into its life cycle. However, at the time of the 1742 UTC warning, the storm was only about an hour into its life from the first 40 dBZ core (not shown). Based on the lapse rate environment and the information in this study, that suggests this first tornado warning was probably issued too soon in the storm's lifetime.

This early supercell storm and another young storm to its southeast (not shown) never did produce tornadoes, although at least four tornado warnings were issued for both supercells before either was two hours old from their initial 40 dBZ cores. As it turns out, none of the supercell storms that developed over the southern U.S. that afternoon produced tornadoes until after three to four hours into their life cycles from an initial 40 DBZ core.

c. 29 April 2022 Andover, KS tornado

This case was discussed briefly in section 2 illustrating methodology. Fig. 4 showed that the supercell producing an EF3 tornado at Andover, KS (causing three injuries, see Fig. 16) took only around 1-1/2 hours to generate a tornado after its initial 40 dBZ core. Fig. 6 in section 2 also showed low-level lapse rates over south-central Kansas associated with this storm. Note that,

Figure 16. EF3 tornado at Andover in south-central Kansas on 29 April 2022. Three people were injured. Video image by Marc Millsap.

compared to the prior two cases above, 0–3-km lapse rates in Fig. 6 were *much steeper* (around 7.5° C km^{-1}), suggesting a shorter lead time from notable radar core to tornado for this tornadic supercell when consulting the Plains section of Table 1.

In this case, there was little advance warning, as the tornado touched down southwest of Andover around 0110 UTC (30 April 2022) at the same time as the initial tornado warning, although significant rotation for this cell on radar began by 0050 UTC (not shown). In contrast to the prior cases examined in this section, this case suggests that when low-level lapse rates are relatively steep given the geographical location, warning meteorologists should be prepared to issue tornado warnings promptly and relatively soon in a supercell's life cycle.

d. 12 April 2022 central Texas tornado

This is an additional example of a supercell that produced a significant tornado relatively fast, similar to the Andover, KS case above.

On 12 April 2022, an EF3 tornado (see Fig. 17) occurred in central Texas northwest of Jarrell. On radar, a 40 dBZ core initially appeared around 2110 UTC (Fig. 18a) near the south end of a cluster of storms between Fort Worth and Austin. At about the time of Fig. 18b (2228 UTC), the EF3 tornado developed from this supercell west of the town of Salado, injuring 23 people. In this case, as in the Andover case, the lead time from notable radar core to tornado was only about 1-1/2 hours.

Figure 17. EF3 tornado west of Salado in central Texas on 12 April 2022. Twenty-three people were injured. Video image by Bobby Eddins.

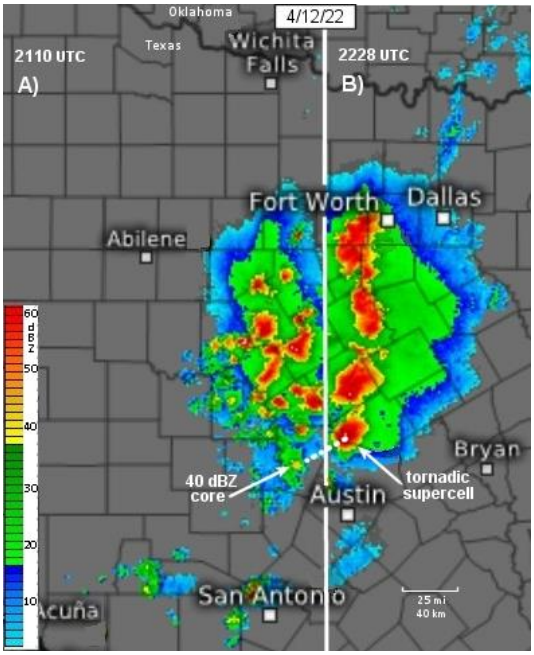

Figure 18. Composite radar reflectivity mosaic as in Fig. 13, except over central Texas on 12 April 2022 at a) 2110 UTC, and b) 2228 UTC. Tornado in Fig. 17 first developed at about the time of b).

Figure 19 (next page) shows the 0–3-km lapse rate field from the SPC mesoanalysis at about the time of the storm's first 40 dBZ core in Fig. 18a (see black square in Fig. 19). Low-level lapse rates were quite steep, in the 9.0 to 9.5° C km^{-1} range over central TX. Again, this is consistent with Table 1, suggesting the potential for relatively rapid tornado development in this Plains case once significant storm rotation began on radar around 2200 UTC (not shown; a tornado warning was issued at 2222 UTC).

e. Other cases of note

Some highlights and comments regarding other cases in this study will be briefly noted here without graphics due to space limitations.

The shortest tornado lead time from initial cell to tornado in the database occurred with a rapidly developing supercell storm in central North Dakota on the afternoon of 15 August 2022 at the eastern edge of the High Plains. The tornado lead time was only roughly 30 minutes in an environment with steep 0–3-km lapse rates (from 8.0 to 9.0° C km^{-1}), which may in part explain this supercell's fast evolution from initiation to generation of an EF2 tornado. However, an additional contributing factor likely

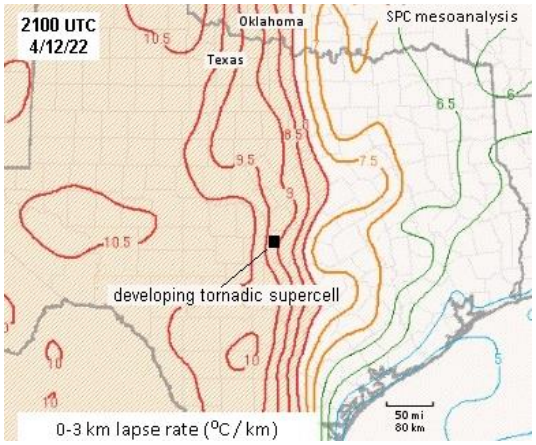

Figure 19. 0–3-km lapse rate as in Fig. 6, except over central Texas on 12 April 2022 at 2100 UTC, corresponding approximately to time of radar in Fig. 18a.

had to do with the supercell's formation directly on a sharp wind shift boundary near the intersection of a cold front and surface trough in this steep low-level lapse rate environment. That suggests this setting may have also included some non-mesocyclone tornado processes (e.g., Caruso and Davies 2005; Davies 2006a; Wakimoto and Wilson 1989).

In the eastern U.S. from the Mississippi Valley eastward where elevation is generally small, low-level lapse rates steeper than 6.5° C km^{-1} within settings that support tornadoes do not appear to occur that frequently. Only 11 of 50 eastern U.S. tornado cases in this study had mean 0–3-km lapse rates $\geq$ 6.5° C km^{-1}. One case in Alabama on the evening of 30 March 2022 featured a large long-track tornado that developed from a supercell embedded in a broad area of rain, and was associated with 0–3-km lapse rates of 6.5 to 7.0° C km^{-1} collocated with an area of large low-level wind shear. This uncommonly steep low-level lapse rate environment (for the southeastern U.S.) likely contributed to this EF3 tornado (and an EF2 tornado shortly before it) that occurred relatively rapidly for this geographical area, between 1.5 and two hours into its parent supercell's life cycle.

Tornadoes associated with mid-level lows (Davies 2006b) often develop rather quickly from low-topped supercells to the northeast, east, or southeast of the mid-level low. With cold air aloft centered in the lower mid-levels accompanying such systems, low-level lapse rates are often steep in these settings, particularly when surface heating east or southeast of the associated surface low is strong. Of 15 "cold-core" tornado cases included in this study, the average mean 0–3-km lapse rate was 6.7° C km^{-1}, and five cases were associated with low-level lapse rates > 7.0° C km^{-1}. These relatively steep lapse rates may help explain the comparatively fast formation of tornadoes in many cold-core cases, sometimes only an hour or so into a low-topped supercell's lifetime, despite narrow or limited axes of moisture and instability near the surface low.

5. Concluding Discussion

With only a little over 100 cases, this study is far from a "climatology" of tornadic supercells and low-level lapse rates. Nevertheless, enough radar and environmental data was accumulated over a year's time to see that there is some noteworthy association between 0–3-km lapse rates and how quickly a developing supercell within a setting supporting supercell tornadoes (e.g., sizable combinations of instability and wind shear) may go on to produce tornadoes. Figure 8 illustrates this.

Additionally, when geographical location and the tendency for low-level lapse rates to be steeper with rising elevation is considered (Fig. 9), this study provides useful information (e.g., Fig. 10, Fig. 11, and Table 1) that might be applied to timing of tornado warnings in differing areas of the U.S.

From the data in Figs. 10 and 11, when supercells go on to produce tornadoes east of the High Plains (i.e., east of 100° W longitude), it typically takes around two hours or more from a storm's first 40 dBZ radar core for a supercell to produce a tornado. This is particularly true in the eastern third of the U.S. where tornado lead times after the first notable radar core are often in the 2.5 to four hour range or greater.

Key exceptions to this (e.g., the relatively rapid development of tornadoes discussed in sections 4c and 4d) tend to involve 0–3-km lapse rates greater than around 6.5° C km^{-1}, and especially low-level lapse rates that approach 7.0 °C km^{-1} and greater. Because low-level lapse rates are typically quite steep due to elevation in the High Plains of the U.S., tornadic supercells in that region tend to produce tornadoes the fastest of the U.S. areas examined in this study.

Application of results from this study is especially pertinent to the early stages of tornado episodes or outbreaks. Again, the Mayfield, KY tornado during the historic 10 December 2021 outbreak is a good example. In that case, an early false alarm tornado warning hours before a large killer tornado struck Mayfield may have influenced supervisors at a candle factory (and possibly other residents of the town) to view a tornado warning hours later less seriously, with potentially deadly consequences. Based on the information from this study, the false alarm tornado warning of a newly-formed storm hours earlier perhaps could have been avoided with knowledge and awareness of the low-level lapse rate environment during the initial warned storm's early lifetime.

A few tornadic supercells in this study, mostly located in the eastern U.S., took five to eight hours into their lifetimes to produce tornadoes. These longer lead times are probably due to a number of factors that are difficult if not impossible to account for, such as interactions with surrounding storms, environments traversed by storms that exhibit varying amounts of instability, low-level shear, and other background characteristics, and of course our limited knowledge of tornadoes and tornadogenesis.

The main goal of this empirical research was to determine whether low-level lapse rates seem to play a role in how fast tornadic supercells produce tornadoes, and whether that information might be applied to tornado warning decisions. The results here certainly suggest an affirmative answer to both questions.

Future research might focus on more detailed radar data to define and examine ”tornado lead time.” For example, the amount of time from a supercell's *first rotational characteristics* on radar to the first tornado produced (instead of using the appearance of a 40 dBZ reflectivity core as the starting point) could be examined in varying low-level lapse rate settings. Wind shear environments associated with low-level lapse rate settings might also be explored to see if background settings with larger low-level wind shear are associated with faster tornado generation in tornadic supercells when 0–3-km lapse rates are generally similar.

In conclusion, the association and variability of supercell tornado lead times found in this study related to low-level lapse rates and geographical location (based roughly on surface elevation) is a compelling finding. In particular, the approximation of *minimum* tornado lead time (i.e., first 40 dBZ radar echo to first tornado) from low-level lapse rate environment and geographical location (e.g., High Plains and central Plains compared to eastern U.S.) appears to have practical application. This is especially true in the early stages of supercell tornado outbreaks and episodes where too many "false alarm" warnings might affect public perception of urgency with potentially deadly results, as suggested by the 2021 Mayfield, KY case. The information from this study should be useful to meteorologists responsible for issuing tornado warnings in such situations.

ACKNOWLEDGMENTS

The author is grateful to my wife Shawna Davies for support and helpful discussion about this project, and for proofreading and suggestions to improve flow and clarity of the manuscript. Thanks go to Mike Smith (Mike Smith Enterprises) for discussion about the Mayfield, KY tornado case. The author also thanks Brett Adair (Live Storms Media), Bobby Eddins, Eddie Knight, and Marc Millsap for the use of their images.

REFERENCES

Bothwell, P. D., J. A. Hart, and R. L. Thompson, 2002: An integrated three-dimensional objective analysis scheme in use at the Storm Prediction Center. Preprints, *21st Conf. on Severe Local Storms*, San Antonio, TX, Amer. Meteor. Soc., J117–J120.

Caruso, J. M., and J. M. Davies, 2005: Tornadoes in non-mesocyclone environments with pre-existing vertical vorticity along convergence boundaries. *NWA Electronic J. Oper. Meteor*., **6**, 1–36. Available online at: http://nwafiles.nwas.org/ej/pdf/2005-EJ4.pdf.

Davies, J. M., 2006a: Tornadoes in environments with small helicity and/or high LCL heights. *Wea. Forecasting*, **21**, 579–594.

_____, 2006b: Tornadoes with cold core 500-mb lows. *Wea Forecasting*, **21**, 1051–1062.

El-Bawab, N., 2021: Workers of candle factory destroyed in tornadoes file class-action lawsuit against company. https://abcnews.go.com/Business/candle-factory-workers-forced-work-tornado-lawsuit/story?id=81789346 (accessed January 20, 2023).

Hampshire, N. L., R. M. Mosier, T.M. Ryan, and D.E. Cavanaugh, 2017: Relationship of low-level instability and tornado damage rating based on observed soundings. *J. Operational Meteor*., **6**, 1–12. Available online at: https://www.spc.noaa.gov/publications/mosier/2018-JOM1.pdf.

Hampton, D., 2021: Factory workers threatened with firing if they left before tornado. https://www.nbcnews.com/news/us-news/kentucky-tornado-factory-workers-threatened-firing-left-tornado-employ-rcna8581 (accessed January 20, 2023).

National Weather Service, 2023: Jet stream - an online school for weather: Radar images: reflectivity. https://www.weather.gov/jetstream/refl (accessed January 20, 2023).

Smith, M., 2021: The tornado warning system failure at Mayfield, Kentucky. http://www.mikesmithenterprisesblog.com/2021/12/the-tornado-warning-system-failure-at.html (accessed January 20, 2023).

Storm Prediction Center, 2023: SPC mesoscale analysis pages. https://www.spc.noaa.gov/exper/mesoanalysis (Accessed January 20, 2023).

Thompson, R. L., R. Edwards, and C. M. Mead, 2004: An update to the supercell composite and significant tornado parameters. *22nd Conf. on Severe Local Storms*, Hyannis MA, Amer.Meteor. Soc., P8.1.

Wakimoto, R. M., and J. W. Wilson, 1989: Non-supercell tornadoes. *Mon. Wea. Rev*., **117**, 1113–1140.